

Propagation Delay and Loss Analysis for Bacteria-based Nanocommunications

V. Petrov, *Student Member, IEEE*, D. Moltchanov, I.F. Akyildiz, *Fellow, IEEE*,
Y. Koucheryavy, *Senior Member, IEEE*

Abstract—Flagellated bacteria have been suggested as one of the techniques to deliver information at nanoscales due to their ability to store massive amounts of data in their DNA strands and their mobility properties. In this paper, the propagation delay and message loss rates are mathematically derived for bacterial nanocommunications. The mobility pattern of the flagellated bacteria is investigated and a stochastic model of the bacteria mobility is developed. The proposed model is then used to derive the performance metrics of interest such as the link reliability as well as the propagation delay distribution for the case where N bacteria are used to deliver the message between two nanomachines. Our solutions reveal that at communication distances inherent for bacteria-based nanonetworks ($1 \sim 10$ mm) reliable links can be established using just few hundreds of bacteria. The presented approach provides the so-far missing analytical building block for performance analysis of prospective bacteria-based nanonetworks.

Index Terms—Nanocommunications, bacteria nanonetworks, channel modeling, propagation delay.

I. INTRODUCTION

Nanotechnology opens the door to the design and manufacture of devices in a scale from one to a thousand nanometers [1]. These nanomachines are capable of computing, sensing and storing operations at the nano level. They can also establish connections between each other to enable data exchange and coordination among them, thus creating a nanonetwork. The capabilities and applications of nanonetworks will rapidly exceed the functionality of a single nanomachine, both in terms of range and complexity [2]. By unifying forces of many nanomachines, nanonetworks can assist in variety of applications, from health and environment monitoring [3], [4] to targeted drug delivery [5].

One of the promising enabler techniques considered for prospective nanonetworks is to utilize flagellated bacteria as information carriers [6]. Bacteria-based nanonetworks can be applied for delay-tolerant communications between bio-inspired nanomachines in a liquid medium. At the same time, the use of bacteria for communications raises many unique challenges that do not exist in electromagnetic-based

nanonetworks [7]. One of the key challenges in bacteria-based nanonetworks is to characterize how random swimming and tumbling of flagellated bacteria affect the performance of the network in terms of link reliability, communication range, and end-to-end delay. To derive these performance metrics, the mobility of bacteria must be analyzed in terms of the probability of free swimming bacteria reaching the destination (e.g., a nanomachine) within a certain amount of time.

To address this objective, many analytical and simulation approaches have been proposed so far. Initial investigations on this problem were performed in [8], where the end-to-end delay was decomposed into encoding, encapsulation, propagation, decapsulation, and decoding delays. Noticing that the propagation delay contributes the most to the end-to-end delay, they studied the propagation delay in depth by a set of numerical values obtained from simulations. The physical layer of bacteria-based nanonetworks was further investigated in [9], with the propagation delay being also evaluated using a simplified simulation tool for bacteria mobility. Later, a thorough simulation model for bacteria-based communications was presented in [10]. Since the detailed simulation of bacteria-based nanonetworks is extremely time-consuming and requires extensive computational power [11], the papers discussed above assumed a limited amount of swimming bacteria (up to few hundreds). On the contrast, the number of bacteria in real environment can reach even millions. Accordingly, an accurate simulation model is also still missing.

On the other hand, the accuracy of the analytical models proposed in [12] and [13] is not feasible due to many simplified assumptions in bacteria mobility process. None of these models takes into account realistic free swimming and tumbling process of flagellated bacteria. Instead, the results in [13] are obtained by approximating the bacteria mobility pattern with random walk over a lattice grid, while the entire message delivery process in [12] is replaced by a random variable that follows a Gamma distribution. Summarizing, the papers discussed above either utilized computationally-expensive simulation tools, or made unrealistic assumptions for the bacteria mobility. Thus, an accurate and scalable framework for performance evaluation of bacteria-based nanonetworks has not been proposed yet.

In this paper, we study the above open problems and develop a new stochastic model capturing the bacteria swimming and tumbling movement process. To obtain the input parameters for our stochastic model, we use a bacteria mobility pattern based on wetlab experiments [14] as a reference. For the sake of the analysis tractability, we make few simplified assump-

Vitaly Petrov, Dmitri Moltchanov, Ian F. Akyildiz, and Yevgeni Koucheryavy are with Nano Communications Center, Department of Electronics and Communications Engineering (TUT-NCC), Tampere University of Technology, Tampere, FI-32720, Finland. Email: vitaly.petrov, dmitri.moltchanov, ian.akyildiz@tut.fi, yk@cs.tut.fi

Ian F. Akyildiz is also with Broadband Wireless Networking Lab, School of Electrical & Computer Engineering, Georgia Institute of Technology, Atlanta, GA 30332, USA. Email: ian@ece.gatech.edu

This work was supported by the FiDiPro program of Academy of Finland "Nanocommunication Networks", 2012—2016.

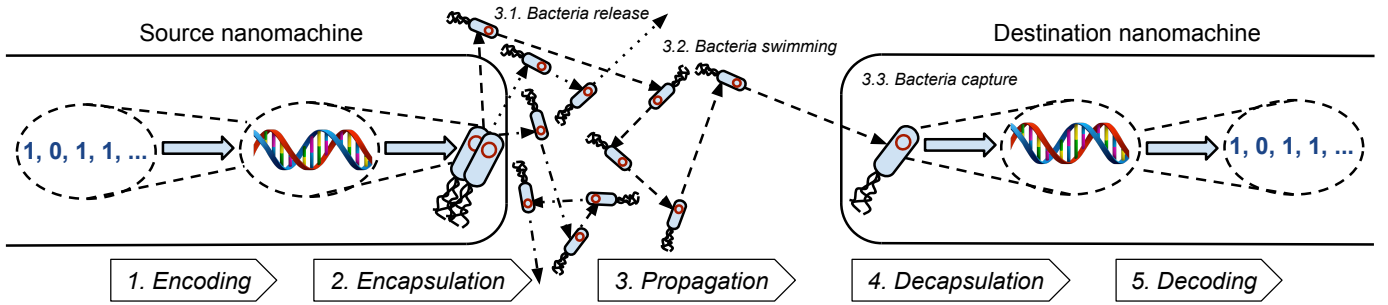


Fig. 1. Communication process in bacteria-based nanonetworks.

tions on the bacteria mobility pattern. Therefore, the developed stochastic model provides a first-order approximation for the realistic bacteria mobility pattern, rather than a completely accurate model. We then formalize our stochastic model of bacteria mobility as a random walk in an unbounded two-dimensional space to predict bacteria location at a certain moment of time. In contrast to previous studies [6], [15] that assume an artificial scenario with a substantial amount of chemo-attractant released by a nanomachine in a certain location and attracting swimming bacteria, we evaluate the bacteria behaviour in natural environment, where chemo-attractant is not present at all or distributed more or less uniformly [14]. Thus, the bacteria mobility pattern is unbiased in our work.

We show that the successful message delivery probability can be calculated in terms of quantiles of the First Passage Time (FPT) distribution in our random walk model. We further determine the propagation delay distribution and the link reliability from the distribution of FPT. The obtained performance measures provide an important block for performance evaluation of bacteria-based nanonetworks. The proposed analytical model can be applied for:

- Faster performance evaluation of bacteria-based nanonetworks instead of time-consuming simulations;
- Estimation of the sufficient quantity of bacteria for the wetlab experiments on bacteria-based nanocommunications;
- Dynamic rate control in bacteria-based nanonetworks by pre-computing the "Conditions (distance, delay, reliability, etc.) / Quantity of bacteria to release" table and storing it on nanomachines.

The remainder of the paper is organized as follows. In Section II, we present the concept of bacteria-based nanonetworks and the performance metrics of interest in our analysis. In Section III, we introduce and analyze the stochastic model of bacteria mobility that is capable of predicting the bacteria location over certain time after release. In Section IV, we apply this model to derive the link reliability and the distribution of the propagation delay. In Section V, we first validate the proposed stochastic model using our simulation framework. We then present the numerical results for the link reliability and the propagation delay under realistic assumptions. Finally, we study the communication range in bacteria-based nanonetworks. We conclude the paper in Section VI.

II. BACTERIA-BASED NANONETWORKS

In this section, we recall the general architecture and summarize major features of bacteria-based nanonetworks, following [6], [8] and other works. We then briefly mention the possible approaches to implement the major stages of communication process. We then describe the performance metrics we concentrate on in our analysis.

A. General Architecture

Bacteria-based nanonetworks consist of *nodes* and *carriers*. Nodes are nanomachines that perform sensing, computing or data storing tasks. The design of prospective nanomachines suggests them to be on a scale of a hundred nanometers and consist of sensors, actuators, processing and storage units, power units with optional energy scavengers, transmitters and receivers for communication purposes [16].

Carriers in bacteria-based nanonetworks are flagellated bacteria, capable of: 1) picking up and releasing DNA molecules through *conjugation* [17] or *transformation* [18]; 2) storing DNA molecules inside the bacterium in the form of *plasmids* or integrating them into bacterium DNA as segments of the *chromosome* [19]; and 3) swimming over the surface of tissue or liquid using *flagella* [14].

The message in bacteria-based nanonetworks has to be represented in the form of a DNA molecule before the transmission. Therefore, the transmitter in a nanomachine should be able to encode the message from the internal nanomachine representation into a sequence of DNA [20]. At the same time, the receiver in a nanomachine should have the ability to decode the message from the DNA sequence into a form that enables further storing or processing of the received data [8].

Depending on the application, the nanomachine either has a set of flagellated bacteria inside [15] or relies on the flagellated bacteria that already exist in the medium. In the first case, the nanomachine uses its bacteria for communication purposes one by one or group by group until the set is over. Once this happens, the nanomachine cannot transmit messages anymore. The presented approach is suitable for the so-called *nanosensors* — nanomachines that perform sensing of some dangerous chemicals and transmit rarely (only when the particular chemical is found).

In the second case, the nanomachine simply emits a number of DNA molecules during the transmission [21]. These molecules will be randomly picked up by swimming bacteria

and eventually delivered to the destination. For consistency of performance metrics definition, in this paper we consider only the first type of nanomachines in our nanonetwork.

B. Communication Process

As suggested in [8], the communication process in bacteria-based networks can be decomposed into five phases, see Fig. 1. Depending on the particular application and type of nanomachines, some of the phases might be modified or even avoided (for instance, encoding for nano sensing and decoding for targeted drug delivery):

- *Encoding*. During this phase, the messages is encoded into a DNA molecule in the source nanomachine. The DNA molecule with the message is replicated to enable encapsulation into a set of bacteria. Use of multiple bacteria instead of a single one increases the chances of the message being successfully delivered to the destination nanomachine during the propagation phase. From the practical perspective, the first generation of nanomachines, capable of bacteria-based nanocommunications, is envisioned to avoid any sophisticated encoding process. On the contrary, they might store a pre-defined set of messages already encoded into plasmids. These plasmids are to be stored in the compartments capable to open in response to an external signal (sensing particular chemical, etc.). The examples of the compartments with abovementioned abilities are given in [22] and [23].
- *Encapsulation (modulation)*. During this phase, the released plasmids with the message are picked up by the carriers (flagellated bacteria) through the process of transformation [18]. Alternatively, a single DNA molecule can be picked up by a bacterium and then spread among the other carriers through the process of conjugation [15].
- *Propagation*. During this phase, bacteria with DNA-encoded messages are released from the source nanomachine, propagate through the medium and, finally, reach the destination nanomachine, where they get captured.
- *Decapsulation (detection)*. During this phase, the envisioned bio-inspired destination nanomachine [25] establishes a pili connection with the captured bacteria to receive a copy of the plasmid with the DNA encoded message through the process of conjugation [15].
- *Decoding*. During this phase, the message is decoded from the received DNA molecules and can be either stored or interpreted by the destination nanomachine. Similar to encoding process, existing level of technologies limits the possibility to decode the DNA sequences by artificial nanomachines. Meanwhile, the bio-inspired nanomachines [24], [25] can apply the natural DNA interpretation techniques to, for instance, synthesize certain proteins depending on the received message. Alternatively, the destination nanomachine can simply be a storage for bacteria with DNA encoded messages from a number of nanosensors [21].

According to [9], the propagation phase in bacteria-based nanonetworks for the distances of few millimeters can last for tens of minutes and even hours; its duration contributes a lot

to the total end-to-end delay. Therefore, in the next section, we thoroughly describe the propagation phase in more detail and also explain the scenario that is analyzed in the paper.

C. Bacteria Propagation

The propagation phase contributes the most to the delay and losses in bacteria-based nanonetworks [8]. Therefore, in this paper we particularly focus on the propagation phase analysis. We consider that encoding/encapsulation phases are performed successfully by the source nanomachines and after the encapsulation phase the source nanomachine has a set of N flagellated bacteria, containing the DNA molecules with the message. Based on these conditions, we formulate the propagation process as a sequence of three steps, see Fig. 1. First, source nanomachine releases N flagellated bacteria, each carrying a copy of the DNA-encoded message. Further, flagellated bacteria propagate through the medium following their swimming pattern. At the final step, once at least one of the bacteria with the message reaches the destination nanomachine, the message is successfully delivered and the propagation phase ends.

In the rest of the paper, we analyze the following single-link scenario. One source and one destination nanomachines are located at distance d from each other. The destination nanomachine is considered static during the entire propagation phase, however, slight movements of the nanomachine do not affect the communication process. To assess a general case, we consider that bacteria swim over the two-dimensional unbounded surface (e.g., a tissue). This condition implies that the area dimensions are much bigger than the distance d .

D. Performance Metrics

We focus on two metrics as part of our analysis:

- *Propagation delay*, D , is defined as the time interval between the bacteria being released from the source nanomachine until at least one of the released bacteria reaches the destination nanomachine.
- *Link reliability*, ρ , is defined as the probability of messages being successfully delivered from the source nanomachine to the destination nanomachine within the given time interval T . With respect to all the released bacteria carrying identical messages, the link reliability equals to the probability of at least one of the bacteria released from the source nanomachine reaching the destination nanomachine within the defined time interval.

Both metrics highly depend on the characteristics of bacteria propagation through the medium. To derive them, we describe and analyze the stochastic model of bacteria mobility.

III. STOCHASTIC MODEL OF BACTERIA MOBILITY

To assess the performance of bacteria-based nanonetworks, the process of bacteria mobility must be first understood. In this section, we first describe the mobility of flagellated bacteria. Based on this, we then formulate our stochastic model of bacteria mobility. Finally, we derive the occupation probability distribution of swimming bacteria that is the key for performance evaluation of bacteria-based nanonetworks.

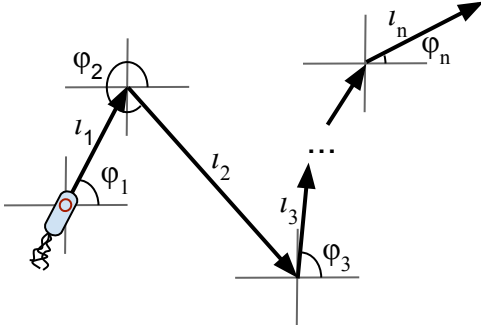


Fig. 2. Empirical pattern of bacteria mobility.

A. Bacteria Mobility

In our study, we focus on the characteristics of *E. Coli* bacterium as one of the most well-investigated flagellated bacterium. As we study the bacteria-based communications in case of chemo-attractant being not present or uniformly distributed, we accept the hypothesis for *E. Coli* mobility in the absence of chemo-attractant, formulated in [14], [26]. According to it, *E. Coli* moves over the surface in the so-called runs and tumbles. In other words, a bacterium alternates swimming in a straight line with short tumbles to select a new direction (see Fig. 2). In the absence of chemo-attractant the selected new angle follows a uniform distribution from 0 to 2π . The speed of swimming bacteria is constant, $v = 20\mu\text{m/s.}$, while the straight swimming time is exponentially distributed with mean $\tau = 3.5\text{s.}$ The latter results in exponentially distributed swimming distances.

Unfortunately, predicting bacteria location after a certain amount of time even for the simplified mobility pattern is complicated. Observe that the unbiased random walk in any dimension is Markov in nature [27]. For one-dimensional space all the states are recurrent positive implying that the process returns to the initial point with probability 1 and the associated mean recurrent time is finite. However, in two-dimensional space the states of the process are all recurrent null and, although the process still returns to the origin with probability 1 the mean recurrence time is infinite. Therefore, it is very difficult to estimate how much time it takes the bacterium to reach the destination nanomachine. In fact, to characterize this metric we have to obtain its distribution. As a result, the derivation of the propagation delay and link reliability metrics is not straightforward. To solve this problem, in the following subsection we propose a stochastic model of bacteria mobility. It is further demonstrated in Section III-C that the proposed model accurately matches the empirical pattern of bacteria mobility starting from tens of seconds. Moreover, the analysis of the model in terms of propagation delay distribution and link reliability is feasible.

B. Stochastic Model Description

In this section, we develop a stochastic model of bacterium mobility over a two-dimension space by deriving a closed-form solution for the probability density function of the bacterium location after release. We demonstrate how the empirical pattern of bacteria mobility can be decomposed

TABLE I
NOTATION USED IN THE PAPER.

Parameter	Definition
v	Bacterium swimming speed
τ	Bacterium mean inter-tumble time
\vec{r}	Coordinates of the destination nanomachine
T	Time since bacteria were released
d	Distance from the center of the source nanomachine to the center of the destination nanomachine
D	Propagation delay (defined in Section II)
ρ	Link reliability (defined in Section II)
n	Amount of bacterium tumbles in $[0, T)$
i	Number of the current tumble
l_i	Length of the i th bacterium run
ϕ_i	New angle selected by the bacterium after tumble i
θ_i	$\pi/4 - \phi_i$
x_i	Projection of l_i on axis OX
y_i	Projection of l_i on axis OY
S_{XY}	Coordinates of the swimming bacterium
S_X	Projection of S_{XY} on axis OX
S_Y	Projection of S_{XY} on axis OY
X	Length of the single run projection on axis OX
Y	Length of the single run projection on axis OY
$E[X], E[Y]$	Mean values of X and Y
$V[X], V[Y]$	Variances of X and Y
μ_x, μ_y	Mean values of S_X and S_Y
σ_x^2, σ_y^2	Variances of S_X and S_Y
$\Phi_Z(\xi)$	Characteristic function of a random variable Z
$\text{erf}(\zeta)$	Error function of argument ζ
$g(\vec{r}, t)$	pdf of the bacterium first passage time to \vec{r}
$G(\vec{r}, t)$	CDF of the bacterium first passage time to \vec{r}
$p(\vec{r}, t)$	Probability of the bacterium being at \vec{r} at time t
$\mathcal{L}(f(x))(s)$	Laplace Transform (LT) of function $f(x)$
$\mathcal{L}^{-1}(F(s))(x)$	Inverse Laplace Transform (ILT) of function $F(s)$
$P(0, s)$	LT of occupation probability for target 0
$P(\vec{r}, s)$	LT of occupation probability for target \vec{r}
$G(0, s)$	LT of first passage time for target 0
$G(\vec{r}, s)$	LT of first passage time for target \vec{r}
p_{XY}	Probability of the bacterium being at the destination nanomachine
p_X	Probability of the bacterium being at the X projection of the destination nanomachine
p_Y	Probability of the bacterium being at the Y projection of the destination nanomachine
k	Skewness of X
γ	Kurtosis of X
α_i	Value of the i th raw moment of X
μ_i	Value of the i th central moment of X
K_n	Kolmogorov's statistics

into a combination of two one-dimensional random processes with known distributions. The following propositions establish stochastic characteristics of the decomposed processes. Table I presents the notation used in the paper.

Proposition 1. *When the amount of bacterium tumbles grows ($n \rightarrow \infty$), the probability density functions of Cartesian coordinates of bacterium location tend to normally distributed random variables S_X and S_Y with means $E[S_X] = E[S_Y] = 0$ and variances $\sigma_X^2 = \sigma_Y^2 = nv^2\tau^2$.*

Proof. We first observe that the tumbling points of the empirical mobility pattern are in fact *regeneration points* of the swimming process. Thus, the direction of the bacterium movement as well as its next run length does not depend on any previous directions or run lengths. We define S_X and S_Y as random variables (RVs) denoting bacterium OX and OY coordinates. Let us also define n to be the number of tumbles the bacterium has performed in the time interval $[0, T)$. In this case, S_X and S_Y can be expressed as

$$S_X = \sum_{i=0}^n x_i, \quad S_Y = \sum_{i=0}^n y_i, \quad (1)$$

where $x_i = l_i \cos(\phi_i)$ and $y_i = l_i \sin(\phi_i)$. In these equations, l_i and ϕ_i represent length of the bacterium run vector and angle the bacterium selects after tumble i .

Since the RVs x_i and y_i , $i = 1, 2, \dots$, are pairwise independent and identically distributed (iid), for sufficiently high i the Central Limit Theorem (CLT) can be applied. Thus, when the number of runs n tends to infinity, S_X and S_Y converge to normal distributions with means $E[S_X] = nE[X]$, $E[S_Y] = nE[Y]$ and variances $\sigma_X^2 = nV[X]$, $\sigma_Y^2 = nV[Y]$. To obtain the expressions for $E[X]$ and $E[Y]$, we first notice that x_i and y_i can be derived by replacing l_i with vt_i , where t_i is a duration of inter-tumbling time and v is bacterium swimming speed

$$x_i = vt_i \cos \phi_i, \quad y_i = vt_i \sin \phi_i. \quad (2)$$

We then recall that, according to Section III-A, t is exponentially distributed with $\lambda = 1/\tau$ and ϕ is uniformly distributed in the range $[0, 2\pi)$. We also note that RVs t and ϕ are independent. Therefore, we obtain $E[X]$ as

$$E[X] = E[vt \cos \phi] = vE[t]E[\cos \phi] = 0 \quad (3)$$

Similarly we get $E[Y] = 0$. These results immediately give

$$E[S_X] = nE[X] = 0, \quad E[S_Y] = nE[Y] = 0. \quad (4)$$

implying that bacterium swimming is *non-biased*.

We then derive $V[X]$ and $V[Y]$. Observe that

$$V[X] = V[vt \cos \phi] = v^2 V[t \cos \phi] = 2v^2 \tau^2 V[\cos(\phi)], \quad (5)$$

where $V[\cos(\phi)]$ is given by

$$V[\cos \phi] = \frac{1}{2\pi} \left(\frac{1}{2} \phi + \frac{1}{4} \sin(2\phi) \right) \Big|_0^{2\pi} = \frac{1}{2}. \quad (6)$$

Substituting the latter to (5) we get $V[X]$ as

$$V[X] = v^2 \tau^2. \quad (7)$$

Similarly, we prove that

$$V[Y] = v^2 \tau^2. \quad (8)$$

Finally, we use (7) and (8) to obtain

$$\sigma_X^2 = nV[X] = nv^2 \tau^2, \quad \sigma_Y^2 = nV[Y] = nv^2 \tau^2. \quad (9)$$

□

The above mentioned result shows that the random variables S_X and S_Y are normally distributed with $E[S_X] = E[S_Y] = 0$ and $\sigma_X^2 = \sigma_Y^2 = nv^2 \tau^2$. The following proposition establishes the independence of the given projections allowing for a simple way of constructing joint probability density function (pdf) from pdfs of the projections.

Proposition 2. *For sufficiently high amount of bacterium tumbles n , S_X and S_Y are independent random variables.*

Proof. To prove the independence of S_X and S_Y , we utilize the mathematical apparatus of characteristic functions (CF). By definition, the CF of a random variable Z is the mean value of $e^{jZ\xi}$,

$$\Phi_Z(\xi) \stackrel{\text{def}}{=} E[e^{jZ\xi}] = \int_{-\infty}^{\infty} f_Z(x) e^{j\xi x} dx. \quad (10)$$

As stated in [28], to show the independence of S_X and S_Y we have to prove the following equation

$$\Phi_{S_X+S_Y}(\xi) = \Phi_{S_X}(\xi) \Phi_{S_Y}(\xi). \quad (11)$$

We first observe that $S_X + S_Y$ can be represented as

$$\begin{aligned} S_X + S_Y &= \sum_{i=0}^n (l_i \cos \phi_i + l_i \sin \phi_i) \\ &= \sum_{i=0}^n l_i \sqrt{2} \cos \left(\frac{\pi}{4} - \phi_i \right). \end{aligned} \quad (12)$$

We also notice, that due to iid nature of summands in (12), the CLT applies when n is sufficiently high, implying that the distribution of $S_X + S_Y$ follows the normal law with mean $E[S_X + S_Y] = nE[X + Y]$ and variance $V[S_X + S_Y] = nV[X + Y]$, where $X + Y = l_i \sqrt{2} \cos(\pi/4 - \phi_i)$.

We then derive the mean and variance of $X + Y$. Recalling the empirical bacteria mobility pattern, ϕ_i is uniformly distributed in $[0, 2\pi)$ implying that $\theta_i = \pi/4 - \phi_i$ is also uniformly distributed in $[0, 2\pi)$. Therefore, we can apply the method from the previous proof to show that $E[X + Y] = 0$ and $V[X + Y] = 2v^2 \tau^2$. This leads to

$$E[S_X + S_Y] = 0, \quad V[S_X + S_Y] = 2nv^2 \tau^2. \quad (13)$$

Thus, the CF of $S_X + S_Y$ can be written as

$$\Phi_{S_X+S_Y}(\xi) = \exp \left(j\mu\xi - \frac{1}{2} \sigma^2 \xi^2 \right), \quad (14)$$

where μ and σ^2 are mean and variance of $S_X + S_Y$.

Substituting (13) into (14) we get

$$\Phi_{S_X+S_Y}(\xi) = \exp \left(-nv^2 \tau^2 \xi^2 \right). \quad (15)$$

Recall that S_X and S_Y follow the normal distribution with $\mu_X = \mu_Y = 0$ and $\sigma_X^2 = \sigma_Y^2 = nv^2 \tau^2$. Therefore,

$$\begin{aligned} \Phi_{S_X}(\xi) \Phi_{S_Y}(\xi) &= \exp \left(j\mu_X \xi - \frac{1}{2} \sigma_X^2 \xi^2 \right) \exp \left(j\mu_Y \xi - \frac{1}{2} \sigma_Y^2 \xi^2 \right) \\ &= \exp \left(-nv^2 \tau^2 \xi^2 \right). \end{aligned} \quad (16)$$

Since right hand sides of (15) and (16) are equal we get

$$\Phi_{S_X+S_Y}(\xi) = \Phi_{S_X}(\xi) \Phi_{S_Y}(\xi). \quad (17)$$

implying that random variables S_X and S_Y are independent. □

In general, a two-dimensional mobility process cannot be fully described by two projections. However, this is possible in our case as S_X and S_Y are independent (see Proposition 2). In Proposition 3 we show how the joint pdf of the bacterium location can be derived from the pdfs of projections.

Proposition 3. *With the growing amount of bacterium tumbles ($n \rightarrow \infty$), the distribution of bacterium occupation probability tends to bivariate Normal distribution with the following joint probability density function:*

$$f_{S_{XY}}(x, y, T) = \frac{1}{2\pi v^2 T \tau} \exp \left(\frac{-x^2 - y^2}{2v^2 T \tau} \right). \quad (18)$$

Proof. The independence of S_X and S_Y by Proposition 2 implies that the joint pdf of the bacterium location $f_{S_{XY}}(x, y, n)$

is equal to the direct multiplication of probability density functions $f_{S_X}(x, n)$ and $f_{S_Y}(y, n)$

$$f_{S_{XY}}(x, y, n) = f_{S_X}(x, n)f_{S_Y}(y, n). \quad (19)$$

At the same time, according to Proposition 1, S_X and S_Y are normally distributed with the following pdfs

$$\begin{aligned} f_{S_X}(x, n) &= \frac{1}{\sigma_X \sqrt{2\pi}} \exp\left(-\frac{x^2}{2\sigma_X^2}\right), \\ f_{S_Y}(y, n) &= \frac{1}{\sigma_Y \sqrt{2\pi}} \exp\left(-\frac{y^2}{2\sigma_Y^2}\right). \end{aligned} \quad (20)$$

Thus, substituting (20) into (19) and approximating T by $n\tau$ for large values of n , we get

$$f_{S_{XY}}(x, y, T) = \frac{1}{2\pi v^2 T \tau} \exp\left(\frac{-x^2 - y^2}{2v^2 T \tau}\right). \quad (21)$$

□

In Proposition 3, we have finally shown that when the amount of bacterium tumbles tends to infinity ($n \rightarrow \infty$), the empirical pattern of bacteria mobility can be well approximated by our stochastic model. In the next subsection, we study how fast the pattern converges to the proposed model.

C. Convergence Rate Study

In this section, we estimate how fast the occupation probability distribution of bacterium location, given by our stochastic model proposed in Section III-B, converges to the one by the empirical bacteria mobility pattern, presented in Section III-A.

Due to the empirical pattern being fully described by a combination of two iid RVs S_X and S_Y , we focus on the convergence of the empirical occupation pdf of S_X , $f_{S_X}^*(x, n)$, and the pdf of S_X from the stochastic model, $f_{S_X}(x, n)$. To illustrate the growing accuracy of our model, we apply the Kolmogorov's statistical test [29].

To perform the Kolmogorov's statistical test, we have to first obtain the closed-form CDFs of both distributions. While the CDF for the stochastic model can be derived by a direct integration of (20), the empirical occupation CDF of S_X has a more complicated form.

In this paper, we apply the results by Levin and Petrov [30], [31], who have made in-depth studies on Central Limit Theorem. In particular, they have shown that the pdf of a sum of n independent identically distributed random variables can be represented as a multiplication of Normal distribution pdf, sum tends to, and weighted sum of Hermite polynomials [32], which tends to 1 for sufficiently large values of n . Thus, according to [30], $f_{S_X}^*(x, n)$ can be written as:

$$\begin{aligned} f_{S_X}^*(x, n) &= \frac{1}{\sqrt{2\pi n \mu_2}} \exp\left(\frac{-(x - n\alpha_1)^2}{2n\mu_2}\right) \left[1 - \frac{k}{6\sqrt{n}} H_3(\omega)\right. \\ &\quad \left. + \frac{\gamma}{24n} H_4(\omega) + \frac{k^2}{72n} H_6(\omega)\right], \end{aligned} \quad (22)$$

where $\omega = (x - n\alpha_1)/\sqrt{n\mu_2}$, $\alpha_1 = E[X]$ — mean of X , $\mu_2 = v^2\tau^2$ — variance of X , $k = \mu_3/(\mu_2\sqrt{\mu_2})$ — skewness of X , $\gamma = \mu^4/\mu_2^2 - 3$ is kurtosis of X , and $H_3(x)$, $H_4(x)$, $H_6(x)$ are the 3rd, 4th and 6th Hermite polynomials, respectively.

Since $\alpha_1 = 0$ and following the properties of random variable central moments [28], μ_3 can be derived as

$$\mu_3 = \alpha_3 - 3\alpha_1\alpha_2 + 2\alpha_1^3 = \alpha_3, \quad (23)$$

where

$$\begin{aligned} \alpha_3 &= E[v^3 t^3 \cos^3(\phi)] = v^3 E\left[t^3 \frac{3\cos(\phi) + \cos(3\phi)}{4}\right] \\ &= \frac{v^3}{4} E[t^3] \left(3E[\cos(\phi)] + E[\cos(3\phi)]\right) = 0. \end{aligned} \quad (24)$$

Thus, $k = 0$. Similarly, μ_4 can be expressed as

$$\mu_4 = \alpha_4 - 4\alpha_1\alpha_3 + 6\alpha_1^2\alpha_2 - 3\alpha_1^4 = \alpha_4, \quad (25)$$

where

$$\begin{aligned} \alpha_4 &= E[v^4 t^4 \cos^4(\phi)] = \frac{v^4}{8} E\left[3E[t^4] + 4E[t^4 \cos(2\phi)]\right. \\ &\quad \left.+ E[t^4 \cos(4\phi)]\right] = \frac{3v^4}{8} E[t^4] = \frac{3\tau^4 v^4}{8} 4! = 9\tau^4 v^4. \end{aligned} \quad (26)$$

Therefore, kurtosis of X is equal to

$$\gamma = \frac{9\tau^4 v^4}{\tau^4 v^4} - 3 = 6. \quad (27)$$

We then substitute the values of $E[X]$ and $V[X]$ from (3) and (7) into (22) to derive $f_{S_X}^*(x, n)$ as

$$f_{S_X}^*(x, n) = \frac{1}{\tau v \sqrt{2\pi n}} \exp\left(\frac{-x^2}{2n\tau^2 v^2}\right) \left[1 + \frac{1}{4n} H_4(\kappa)\right], \quad (28)$$

where $\kappa = x/(\tau v \sqrt{n})$ and $H_4(z) = z^4 - 6z^2 + 3$ [32].

We are now able to apply the Kolmogorov's statistical test. To perform this study, we estimate the maximum difference between the empirical Cumulative Distribution Function (CDF) of S_X , $F_{S_X}^*(x, n)$, and the CDF of S_X given by our stochastic model, $F_{S_X}(x, n)$

$$\begin{aligned} K_n &= \sup_x |F_{S_X}^*(x, n) - F_{S_X}(x, n)| \\ &= \frac{1}{4n\sqrt{\pi}} \sup_x \left| \int_{-\infty}^x \exp(-x^2) (4x^4 - 12x^2 + 3) dx \right| \\ &\leq \frac{1}{4n\sqrt{\pi}} \left(\int_{-\infty}^{\infty} 3 \exp(-x^2) dx + \int_{-\infty}^{\infty} 4 \exp(-x^2) x^4 dx \right. \\ &\quad \left. - \int_{-\infty}^{\infty} 12 \exp(-x^2) x^2 dx \right) = \frac{1}{4n\sqrt{\pi}} (3\sqrt{\pi} + 0) = \frac{3}{4n}. \end{aligned} \quad (29)$$

We now apply the Kolmogorov criterion to K_n . To prove the hypothesis with confidence 0.9999 we need to find the value of n , such that $\sqrt{n}K_n \leq 0.29$ [33]. Using (29), we obtain the minimum value of n as $n_{min} = 7$. Recalling that the average run duration is 3.5s., we conclude that our stochastic model converges to the empirical pattern of bacteria mobility starting from approximately the 25th second. Since the propagation delay in bacteria-based nanonetworks can reach hours [34], the accuracy of the proposed model is absolutely sufficient.

Summarizing, the results provided in this section allow us to decompose the two-dimensional bacteria mobility pattern into a combination of two independent one-dimensional random processes. Further, the location of a bacterium after several runs can be well described by a bivariate Normal distribution $f_{S_{XY}}$, which is a product of two independent one-dimensional

distributions f_{S_X} and f_{S_Y} . We heavily rely on these properties in the following section deriving the propagation delay distribution and the link reliability in bacteria-based nanonetworks.

IV. PROPAGATION DELAY AND LINK RELIABILITY

In this section, we use the stochastic model of bacteria mobility to obtain the propagation delay distribution and the link reliability in bacteria-based nanonetworks. Both metrics can be derived from the distribution of FPT – time interval for the released bacteria to reach the destination nanomachine for the first time. We start this section with revising the technique of getting the distribution of FPT from the occupation probability distribution. We then calculate the probability of the selected bacteria reaching the receiver location at a particular moment of time. Finally, we derive the performance metrics of interest.

A. First Passage Time Derivation Technique

The analysis for FPT in dimensions higher than one is complex even for unbiased discrete random walks with step of size 1 [35]. When continuous jumps are allowed the problem is directly solvable for a limited set of random walks only [27]. The bacterium moving pattern is classified as a modified Pearson-Rayleigh random walk [27]. For this walk, in spite of significant efforts spent over the last century, no result for FPT is available. In fact, any unbiased random walk with jump distribution having finite first two moments is characterized by Normally distributed position of a moving particle [27]. Due to this property, in practical applications unbiased continuous random walks are approximated by Brownian motion with appropriate diffusion constant [36]. For this process the FPT in simple geometries in dimensions higher than one could be found using Green function approach in terms of the Laplace-Stieltjes transform (LST). However, Brownian motion is a special case of position jump processes allowing for infinite propagation distances at infinitesimally small amount of times making them unrealistic for modeling purposes. Below, we derive LST of RDM in \mathfrak{R}^2 .

We recall the FPT derivation methodology given in [36]. The approach is based on the following fact: if the moving object reaches the target \vec{r} second time at time t , it means that this moving object already reached the target \vec{r} at some time $t^* < t$ and then returned to this point exactly after time $t - t^*$. Therefore, there is a connection between the probability density functions of the moving object being at the target location, $p(\vec{r}, t)$, and the moving object reaching the target location for the first time, $g(\vec{r}, t)$:

$$p(\vec{r}, t) = \delta_{\vec{r}0} \delta_{t0} + \sum_{t^* \leq t} g(\vec{r}, t^*) p(0, t - t^*), \quad (30)$$

where $\delta_{\vec{r}0}$ and δ_{t0} are the Kronecker's delta functions.

The distribution of the FPT can be derived from this equation using the Laplace transform [37]. Defining one-sided Laplace transforms of $p(\vec{r}, t)$ and $g(\vec{r}, t)$ as

$$P(\vec{r}, s) = \int_0^\infty p(\vec{r}, t) e^{-st} dt, \quad (31)$$

$$G(\vec{r}, s) = \int_0^\infty g(\vec{r}, t) e^{-st} dt, \quad (32)$$

the (30) can be rewritten in Laplace domain as

$$P(\vec{r}, s) = \delta_{\vec{r}0} + G(\vec{r}, s) P(0, s), \quad (33)$$

immediately leading to the general solution

$$G(\vec{r}, s) = \begin{cases} 1 - \frac{1}{P(0, s)}, & \vec{r} = 0 \\ \frac{P(\vec{r}, s)}{P(0, s)}, & \vec{r} \neq 0. \end{cases} \quad (34)$$

To apply the given technique, the expressions for pdfs of two random variables in Laplace domain have to be derived. First of them is the pdf of a swimming bacterium reaching the destination nanomachine at time t . The second is the pdf of the swimming bacterium returning back to the source nanomachine at time t . In the next section, we derive these densities from our stochastic model of bacteria mobility.

B. Performance Analysis

Based on the stochastic model of bacteria mobility, in this section we derive the propagation delay distribution and the link reliability for bacteria-based nanonetworks. We first evaluate the simplified scenario with a single bacterium released from the source nanomachine and then generalize our results to the scenario described in Section II, i.e. when a set of bacteria are simultaneously released from the source nanomachine.

Following [8], the destination nanomachine is assumed to have a square shape with a side of $100\mu\text{m}$. We derive the probability of the message carrier (bacterium) arriving at the destination nanomachine at time t , $p_{xy}(t)$, as a function of: 1) the distance, d , between centres of source and designation nanomachines, 2) the nanomachine size, $2r$, 3) the average straight swimming time of bacterium, τ , 4) the bacterium swimming speed, v , 5) the time after bacterium release, T .

For a square-shape nanomachine, the probability of the selected bacterium located at (x, y) being at the destination nanomachine at time T can be expressed as

$$p_{xy}(T) = Pr\{x(t) \in [d - r, d + r] \cap y(t) \in [-r, +r] \mid t \in [T, T + dT]\}. \quad (35)$$

Due to independence of bacteria mobility over OX and OY axes (see Proposition 2), $p_{xy}(T)$ can be represented as

$$p_{xy}(T) = p_x(T) p_y(T), \quad (36)$$

where $p_x(T)$ and $p_y(T)$ are the following probabilities

$$p_x(T) = Pr\{x(t) \in [d - r, d + r] \mid t \in [T, T + dT]\}, \\ p_y(T) = Pr\{y(t) \in [-r, +r] \mid t \in [T, T + dT]\}. \quad (37)$$

According to Proposition 3, the occupation probability of the bacterium location follows Normal distribution with $E[X] = E[Y] = 0$ and $\sigma_X^2 = \sigma_Y^2 = n v^2 \tau^2$. Thus, the occupation probabilities for projections are

$$p_x(T) = \int_{d-r}^{d+r} f_{S_X}(x, T) dx = \frac{1}{2} \left[\text{erf} \left(\frac{d+r}{\sigma\sqrt{2}} \right) - \text{erf} \left(\frac{d-r}{\sigma\sqrt{2}} \right) \right], \\ p_y(T) = \int_{-r}^r f_{S_Y}(y, T) dy = \text{erf} \left(\frac{r}{\sigma\sqrt{2}} \right), \quad (38)$$

$$\begin{aligned}
f_D(d, T) &= \frac{1}{2} \mathcal{L}^{-1} \left(\frac{\mathcal{L} \left(\operatorname{erf} \left(\frac{r}{\sqrt{2\tau T}} \right) \operatorname{erf} \left(\frac{d+r}{\sqrt{2\tau T}} \right) \right) - \mathcal{L} \left(\operatorname{erf} \left(\frac{r}{\sqrt{2\tau T}} \right) \operatorname{erf} \left(\frac{d-r}{\sqrt{2\tau T}} \right) \right)}{\mathcal{L} \left(\operatorname{erf}^2 \left(\frac{r}{\sqrt{2\tau T}} \right) \right)} \right) \\
&= \frac{1}{2} \left(\operatorname{erf} \left(\frac{r}{\sqrt{2\tau T}} \right) \left[\operatorname{erf} \left(\frac{d+r}{\sqrt{2\tau T}} \right) - \operatorname{erf} \left(\frac{d-r}{\sqrt{2\tau T}} \right) \right] \right) * \mathcal{L}^{-1} \left(1 / \mathcal{L} \left[\operatorname{erf}^2 \left(\frac{r}{\sqrt{2\tau T}} \right) \right] \right). \quad (42)
\end{aligned}$$

where $\sigma = v^2 \tau T$.

By substitution of (38) into (36) we get

$$p_{xy}(T) = \frac{1}{2} \operatorname{erf} \left(\frac{r}{\sigma \sqrt{2}} \right) \left[\operatorname{erf} \left(\frac{d+r}{\sigma \sqrt{2}} \right) - \operatorname{erf} \left(\frac{d-r}{\sigma \sqrt{2}} \right) \right]. \quad (39)$$

We then apply the linearity property of Laplace transform to simplify the expression for $p_{xy}(T)$ in Laplace domain:

$$P(\vec{r}, s) = \frac{1}{2} \left(\mathcal{L} [\operatorname{erf}(t) \operatorname{erf}(\eta_1 t)] - \mathcal{L} [\operatorname{erf}(t) \operatorname{erf}(\eta_2 t)] \right), \quad (40)$$

where $\operatorname{erf}(\cdot)$ is an error function and

$$t = \frac{r}{\sqrt{2\tau T}}, \quad \eta_1 = 1 + \frac{d}{r}, \quad \eta_2 = 1 - \frac{d}{r}.$$

Similarly, $P(0, s)$ is given by

$$P(0, s) = \mathcal{L} (\operatorname{erf}^2(t)). \quad (41)$$

Finally, using the Inverse Laplace Transform (ILT), the probability density function of the propagation delay can be derived as shown in (42), where T is the time since bacterium release, while d , r , τ , and v are deployment and environmental parameters (see Table I for details).

We also notice that by definition, the link reliability in bacteria-based nanonetworks is equal to the CDF of the propagation delay. Therefore, the link reliability for the simplified scenario — the probability of a single bacterium reaching the target d micrometers far from the source nanomachine within T hours, $\rho(d, T)$, — can be expressed as:

$$\rho(d, T) = F_D(d, T) = \int_0^T f_D(d, t) dt. \quad (43)$$

We now generalize the obtained results for the case, when the source nanomachine emits $N > 1$, bacteria at time $t = 0$ carrying the identical messages. In this scenario, the bacteria movement is assumed to be independent. In practice, this happens when no extensive chemio-attractants are available in the close proximity making the movement unbiased. The link reliability $\rho_N(d, T)$ is then given by

$$\rho_N(d, T) = 1 - [1 - \rho(d, T)]^N. \quad (44)$$

Using the similar technique, the pdf of the propagation delay can be derived as

$$\begin{aligned}
f_{D_N}(d, T) &= \frac{d}{dt} \left(\rho_N(d, T) \right) \\
&= N f_D(d, T) (1 - \rho(d, T))^{N-1}. \quad (45)
\end{aligned}$$

Finally, we estimate the number of bacteria N^* to be released from the source nanomachine to reach a certain reliability level for given values of input parameters d , T and

P_s , where P_s denotes the required reliability value. This can be performed by inversion of (44):

$$N^* = \log_{[1-\rho(d, T)]} (1 - P). \quad (46)$$

Based on (46), a tunable algorithm for the communication in bacteria-based nanonetworks can be proposed. If the distance to the destination nanomachine is known or could be estimated, the source nanomachine can release a certain quantity of bacteria to deliver a particular message (N^*) based on the probability of the message successful delivery (P) — quantitative criterion for the message importance, and the required average propagation delay (T) — quantitative metric for the message delay tolerance. The major trade-offs between the listed parameters are studied in the next section.

V. NUMERICAL RESULTS

In this section, the obtained analytical results are numerically elaborated. We start with validation of our stochastic model of bacteria mobility by comparing its characteristics with the ones observed from the empirical pattern. We then numerically analyze the propagation delay distribution and then link reliability. We also study the quantity of bacteria to be released from the source nanomachine to reach prescribed performance metrics. Finally, we investigate the communication range achievable in bacteria-based nanonetworks.

A. Stochastic Model Validation

Here, we assess the accuracy of our stochastic model proposed in Section III. We first numerically study the convergence rate of our model to the empirical pattern of bacteria mobility. We then present a comparison of occupation probability densities obtained from the model and those of the pattern. Finally, we discuss the applicability of the proposed model to other types of flagellated bacteria (not just *E. Coli*) with different swimming speeds and tumbling rates.

To investigate the convergence rate of our model to the empirical pattern as a function of time after bacteria release, we apply the method presented in Section III-C. Fig. 3(a) presents the results based on (29) for the bacterium mean inter-tumble time, τ , set to 3.5s, as revealed in [26]. As one can observe from this figure, the model converges to the pattern starting from 30s ($\sqrt{n}K_n < 0.29$ with confidence 99,99%) and becomes extremely accurate approximately 5 minutes after release.

We further illustrate the accuracy of the proposed model directly comparing its occupation pdfs with the pdfs of the empirical pattern. To derive the occupation probability densities for the empirical pattern, we have developed a simulator

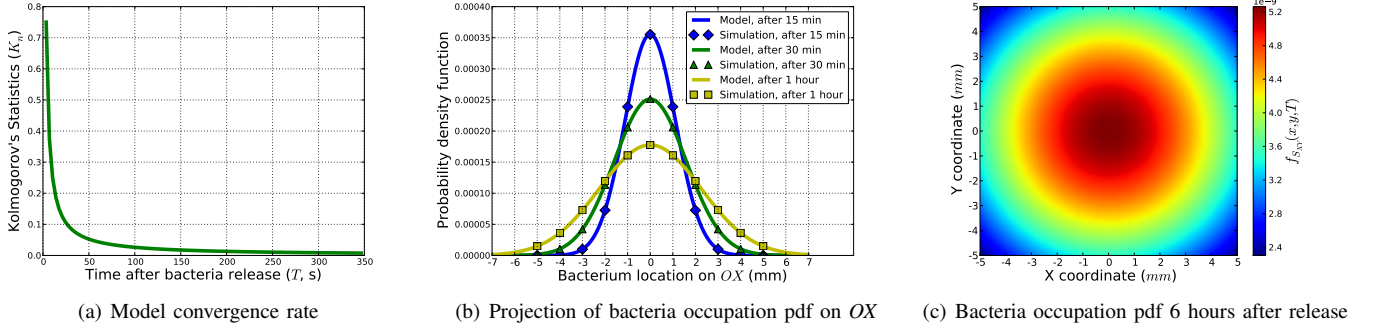


Fig. 3. Validation of the proposed stochastic model.

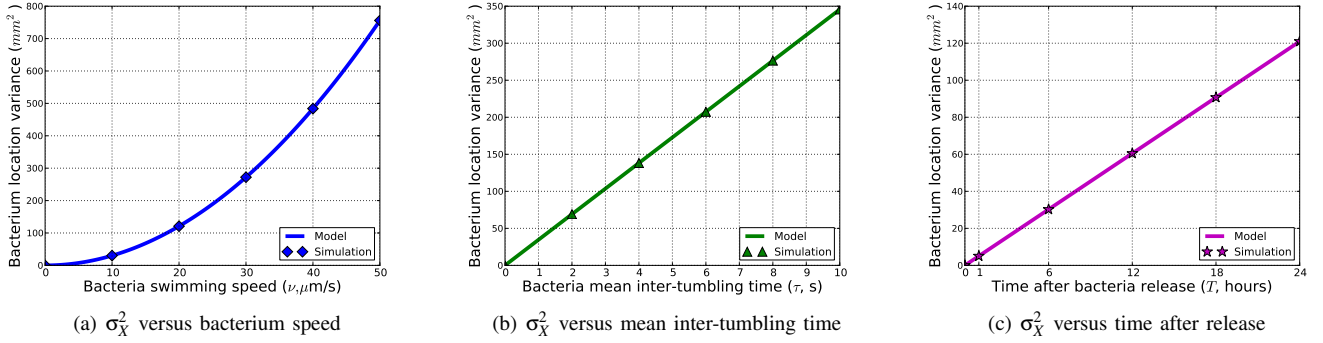


Fig. 4. Variance of the bacterium location on OX as a function of bacteria mobility characteristics.

of bacteria mobility. The simulator works as follows: 1) a set of bacteria is released from point $(0,0)$ at time $0s$; 2) all the released bacteria independently swim over the surface following the empirical pattern, described in Section III-A. 3) after T seconds the experiment ends and current coordinates of the bacteria are combined to form a bivariate pdf and projections of its projections on axes OX and OY .

Fig. 3(b) demonstrates the projection of bacteria occupation pdf on OX . Due to the symmetry of the projections, it is sufficient to consider only one of them. In this figure, blue, green, and yellow curves illustrate the results of (20), 15, 30 and 60 minutes after bacteria release, respectively. Dots in this figure represent the simulation results for the same set of input parameters. Observing the results, one could see a perfect match (less than 1% absolute difference), which is significantly better comparing to the accuracy of lattice-grid-based and Gamma-based approximations (see [11] and [10]). For the selected distributions we also perform the χ^2 homogeneity test with the significance level, $\alpha/2$, set to 0.05 proving our conclusions that two sets of data comes from the same distribution [38]. Thus, we can rely on the model characteristics in further numerical analysis. An example of the bivariate pdf provided by our model, 6 hours after bacteria are released, is shown in the Fig. 3(c).

In addition to the distribution test, we compare the first two moments of the bacterium location projection on OX to find out whether the proposed model converges to the empirical pattern with other numerical values of the bacteria swimming speed, v , bacterium mean inter-tumbling interval, τ , and time after bacteria release, T . To obtain the results for the empirical pattern, we again use our simulation tool. As

one could observe from Fig. 4, the proposed model converges to the empirical pattern regardless the numerical values of bacteria characteristics.

Based on the presented validation results, we conclude that our analysis in Section III-B is correct, and the proposed model can be used to approximate the mobility of any flagellated bacteria that move according to the pattern, described in Section III-A. We apply the model to evaluate the performance of bacteria-based nanonetworks in the next section.

B. Performance Analysis: Single Bacterium Scenario

In this section, we analyze the simplified scenario, where the source nanomachine releases a single bacterium carrying the message. We focus on two metrics of interest, listed in Section II-D: the link reliability and the propagation delay distribution. Due to affordable computational complexity of the scenario, we corroborate our analytical investigations with the simulation results given by our tool from [39].

We start with the results for the distribution of the propagation delay, presented in Fig. 5. The curves in this figure are derived using (42) with the distance, d , varying from 1mm to 5mm, bacteria mean inter-tumbling time, τ , set to 3.5s, and the nanomachine size, $2r$, set to $100\mu m$. To obtain the numerical values of the Inverse Laplace Transform we have applied an improved Talbot's method, described in [40]. This technique is known to be versatile and accurate. As one can note from Fig. 5, the average value, expectedly, increases with the distance. Assessing the match between analytical and simulation results, we observe less than 3% difference. Similarly to the previous section, the performed χ^2 homogeneity test confirms the correctness of the propagation delay analysis, presented in Section IV.

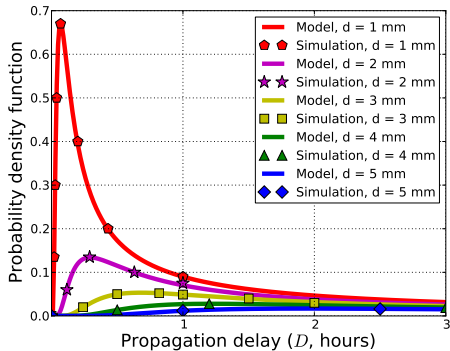


Fig. 5. Single bacterium scenario: propagation delay pdf.

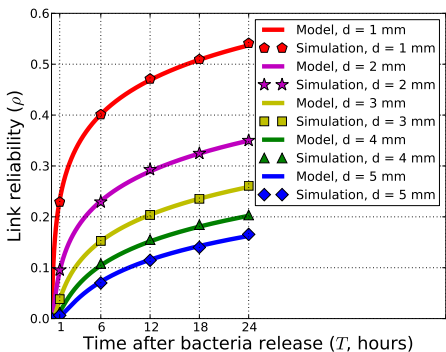


Fig. 6. Single bacterium scenario: link reliability.

It is important to note that the perfect match of the model-based and simulation-based propagation delay distributions facilitates the derivation of the link reliability, presented in Fig. 6. In this figure, the model results are determined by (43). Due to the direct connection between the propagation delay distribution and the link reliability (see Section IV for details), the simulation values are obtained by just numerical integration of the results, presented in Fig. 5. We again observe a good match between the two sets of data (less than 4% difference). In addition, we notice the link reliability constantly decreasing with the growth of the distance between the nanomachines. Moreover, we reveal that within 24 hours after bacterium release the link reliability does not reach 0.6 even for 1mm distance. Therefore, we conclude that reliable communications in bacteria-based nanonetworks cannot be performed using just a single bacterium. In the next section, we investigate if it is possible to improve the characteristic by releasing a set of bacteria instead.

C. Performance Analysis: Multiple Bacteria Scenario

In this section, we study the link behavior, when multiple bacteria are simultaneously released from the source nanomachine. With respect to the increased computational complexity of the scenario, we do not supplement the analytical results with the simulation-based ones. However, the two intermediate verifications performed in Sections V-A and V-B confirm the accuracy of our analysis.

We start our numerical investigations observing the effect of released bacteria quantity on the propagation delay distri-

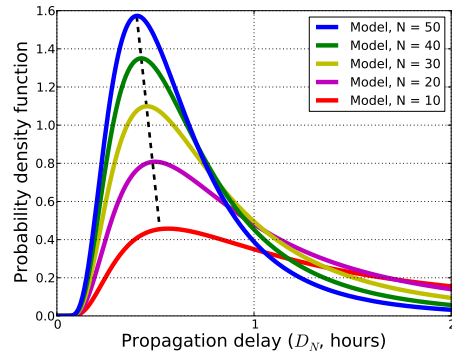


Fig. 7. Multiple bacteria scenario: propagation delay pdf at 3mm.

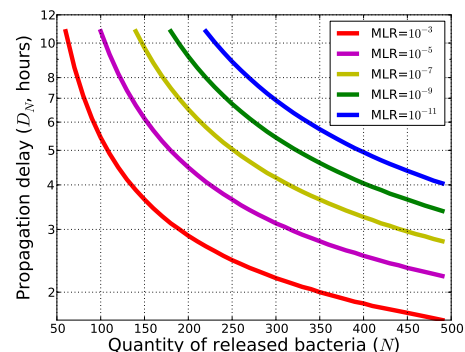


Fig. 8. Multiple bacteria scenario: propagation delay quantiles at 5mm.

bution. Fig. 7 presents the results for this metric computed using (45) with the distance between the source and the destination nanomachines, d , set to 3mm and the number of released bacteria, N , varying from 10 to 50. The peakedness of the density increases and the mode of the propagation delay decreases when N grows. Based on the results, we can expect the link reliability, given by a quantile of the delay distribution, to increase with the number of released bacteria.

To investigate the effect of bacteria population on the link reliability in detail, in Fig. 9, we plot the link reliability as a function of the number of released bacteria for different time instants and distances between the nanomachines, see (43) and (44). As expected, the link reliability decreases with distance and increases in response to the growth in the quantity of released bacteria. Observing these plots, we also detect a straightforward trade-off between the tolerable propagation delay values and the required number of the released bacteria. Thus, if the application is not delay sensitive, the same level of reliability can be reached with exponentially smaller bacteria quantity. In particular, the link reliability of 0.98 can be achieved with 25 times smaller colony of bacteria (40 instead of 1000) if the application can tolerate delay of twelve hours instead of just one, as evident from Fig. 9(a) and Fig. 9(c).

Increasing the quantity of released bacteria, one not only improves the link reliability, but also dramatically decreases the propagation delay value as shown in Fig. 7. Thus, the release of high number of bacteria can also be applied for delay-critical types of traffic. To study this effect rigorously, we introduce the characteristic called *Message Loss Rate (MLR)*

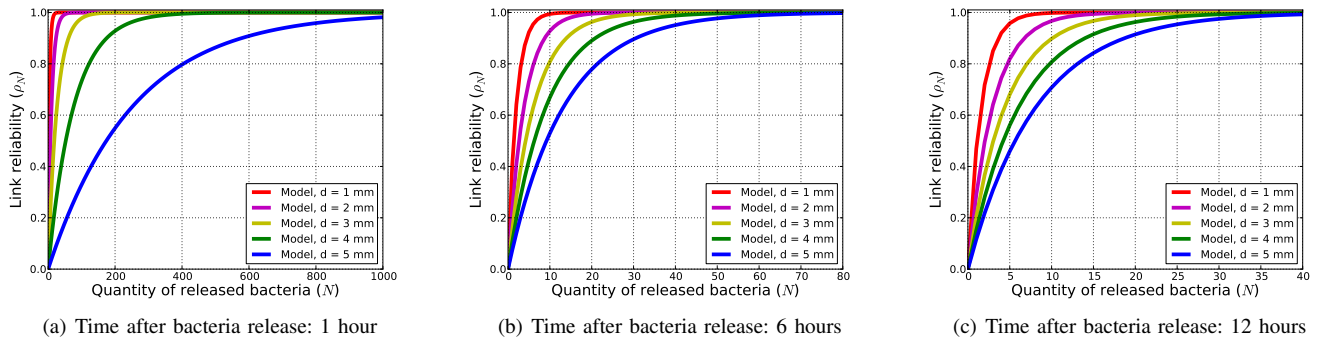


Fig. 9. Multiple bacteria scenario: link reliability versus quantity of released bacteria.

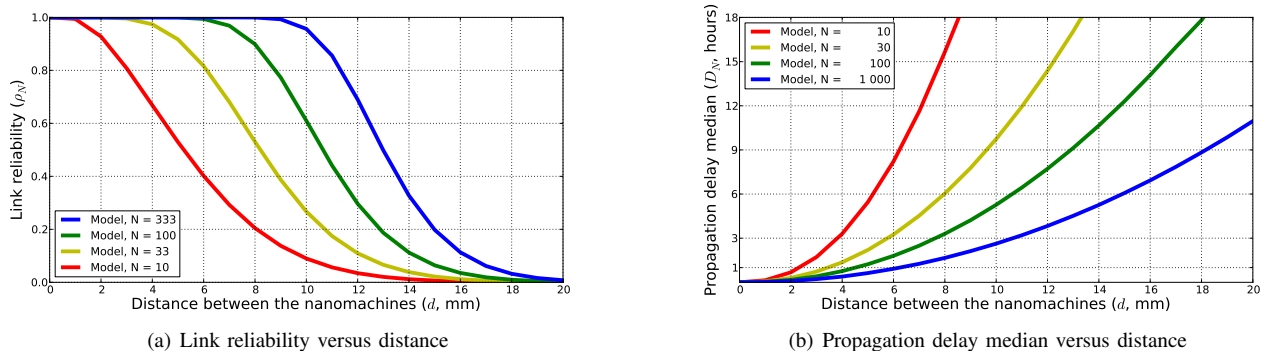


Fig. 10. Multiple bacteria scenario: the effect of distance between the nanomachines.

— the probability that the selected bacterium does not reach the destination nanomachine within the given time. In Fig. 8 we present the propagation delay quantiles corresponding to different MLR values for the various quantities of released bacteria. We see that extremely low values of MLR can be achieved for millimeter distance by emitting just few hundreds of flagellated bacteria.

Finally, we observe the effect of link performance degradation with distance, that is, the decrease in link reliability accompanied by the propagation delay increase. Since the mean delay for our network is infinite due to the nature of our mobility process [27], we illustrate this effect replacing the non-indicative mean value with the median of the delay distribution. We present both the link reliability and the propagation delay median as functions of distance in Fig. 10. As one can observe from Fig. 10(a), the communication range for bacteria-based nanonetworks can reach values up to one centimeter, confirming the predictions, done in [6]. However, Fig. 10(b) shows that the associated delay values will be high.

VI. CONCLUSIONS

Bacteria-based nanonetworks potentially enable a number of promising applications of nanotechnology in environmental and healthcare fields. However, the performance evaluation of bacteria-based nanonetworks is still an unsolved challenge.

In this paper, we have studied the above mentioned problem by performing the propagation delay and link reliability analysis for bacteria-based nanonetworks. To avoid extensive simulations, we have proposed an analytical model for information delivery by flagellated bacteria in unbounded two-

dimensional space. The proposed analytical model presents an attempt to incorporate the bacteria swimming and tumbling mobility pattern in the communication process. Our model is focused on the environment with uniform distribution of chemo-attractant and, for the sake of analysis tractability, incorporates several simplified assumptions on the bacteria mobility pattern (namely, unbiased choice of new direction after tumbling).

Compared to conventional models based on the diffusion approximation of the bacteria mobility process, see e.g. [41], the proposed model by design provides more accurate approximation, especially for short communication distances that are expected to be of special interest in bacterial networks. This is due to diffusion-based models being characterized by infinite propagation speed that significantly affects the propagation time. Notice that when $t \rightarrow \infty$ the first passage time of the proposed model converges to that of the diffusion one [27].

Based on the proposed mathematical framework for bacteria-based nanonetworks, we have provided a complete analysis of the link performance metrics as functions of bacteria mobility pattern, distance between nanomachines, and quantity of released bacteria. Furthermore, we have presented a technique to estimate the number of released bacteria that ensure the prescribed level of the link reliability and the propagation delay. Finally, we have studied the communication range for bacteria-based nanonetworks. We have illustrated that reliable links of up to one centimeter distance can be achieved with only several hundreds of released bacteria. The obtained results provide an important step towards the performance evaluation of bacteria-based nanonetworks.

ACKNOWLEDGEMENT

The authors would like to thank the anonymous reviewers for their valuable comments and suggestions to improve the quality of the paper. The authors are also grateful to Ozan Bicen, Chong Han, Youssef Chahibi, Elias Chavarria Reyes, Hamideh Ramezani, Murat Kuscu, and Ozgur Akan for their constructive feedback.

REFERENCES

- [1] D. M. Smith, J. K. Simon, and J. R. Baker Jr, "Applications of nanotechnology for immunology," *Nature Reviews Immunology*, vol.13, pp. 592–605, Sep. 2013.
- [2] I. F. Akyildiz, J. M. Jornet, and M. Pierobon, "Nanonetworks: A new frontier in communications," *Commun. ACM*, vol. 54, no. 11, pp. 84–89, Nov. 2011.
- [3] N. A. W. Bell and U. F. Keyser, "Digitally encoded DNA nanostructures for multiplexed, single-molecule protein sensing with nanopores," *Nature Nanotech.*, April 2016.
- [4] T. Nakano, M. J. Moore, F. Wei, A. V. Vasilakos, and J. Shuai, "Molecular Communication and Networking: Opportunities and Challenges," *IEEE Trans. NanoBioscience*, vol. 11, no. 2, pp. 135–148, June 2012.
- [5] A. Sahari, M. A. Traore, B. E. Scharf, and B. Behkam, "Directed transport of bacteria-based drug delivery vehicles: bacterial chemotaxis dominates particle shape," *Biomed Microdevices*, vol. 16, no. 5, October 2014.
- [6] M. Gregori and I. F. Akyildiz, "A new nanonetwork architecture using flagellated bacteria and catalytic nanomotors," *IEEE JSAC*, vol. 28, pp. 612–619, May 2010.
- [7] I. F. Akyildiz, F. Fekri, R. Sivakumar, C. Forest, and B. Hammer, "Monaco: fundamentals of molecular nano-communication networks," *IEEE Wireless Comm. Mag.*, vol. 19, pp. 12–18, Oct. 2012.
- [8] L. Cobo and I. F. Akyildiz, "Bacteria-based communication in nanonetworks," *Nanocommunication Networks (NANOCOMNET) Journal, Elsevier*, vol. 1, pp. 244–256, Dec. 2010.
- [9] M. Gregori, I. Llatser, A. Cabellos-Aparicio, and E. Alarcon, "Physical channel characterization for medium-range nanonetworks using flagellated bacteria," *Computer Networks Journal, Elsevier*, vol. 55, pp. 779–791, Feb. 2011.
- [10] W. Guopeng, P. Bogdan, and R. Marculescu, "Efficient modeling and simulation of bacteria-based nanonetworks with BNSim," *IEEE JSAC*, vol. 31, pp. 868–878, Dec. 2013.
- [11] T. J. Rudge, P. J. Steiner, A. Phillips, and J. Haseloff, "Computational modeling of synthetic microbial biofilms," *ACS Synth. Biol.*, vol. 1, pp. 345–352, July 2012.
- [12] D. Arifler, "Link layer modeling of bio-inspired communication in nanonetworks," *Nanocommunication Networks (NANOCOMNET) Journal, Elsevier*, vol. 2, pp. 223–229, Dec. 2011.
- [13] G. Wei, P. Bogdan, and R. Marculescu, "Bumpy rides: modeling the dynamics of chemotactic interacting bacteria," *IEEE JSAC*, vol. 31, pp. 879–890, Dec. 2013.
- [14] Z. Wang, M. Kim, and G. Rosen, "Validating models of bacterial chemotaxis by simulating the random motility coefficient," *In Proc. IEEE BIBE*, Oct. 2008.
- [15] S. Balasubramaniam and P. Lio, "Multi-hop Conjugation based Bacteria Nanonetworks," *IEEE Trans. on NanoBioscience*, vol. 12, pp. 47–59, March 2013.
- [16] I. F. Akyildiz, F. Brunetti, and C. Blazquez, "Nanonetworks: A new communication paradigm," *Computer Networks Journal, Elsevier*, vol. 52, pp. 2260–2279, June 2008.
- [17] M. Achtman, N. Kennedy, and R. Skurray, "Cell–cell interactions in conjugating *Escherichia coli*: role of traT protein in surface exclusion," *Proc. USA Nat. Acad. of Sciences*, vol. 74, pp. 5104–5108, Nov. 1977.
- [18] D. Hanahan, "Studies on transformation of *Escherichia coli* with plasmids," *Journal of Molecular Biology*, vol. 166, pp. 557–580, 1983.
- [19] J. Bonnet, P. Subsoontorn, and D. Endy, "Rewritable digital data storage in live cells via engineered control of recombination directionality," *Proc. USA Nat. Acad. of Sciences*, vol. 109, pp. 8884–8889, Apr. 2012.
- [20] J. Bonnet, P. Subsoontorn, and D. Endy, "Rewritable digital data storage in live cells via engineered control of recombination directionality," *In Proc. of the National Academy of Sciences of the United States of America*, vol. 109, pp. 8884–8889, April 2012.
- [21] V. Petrov, D. Moltchanov, S. Balasubramaniam, Y. Koucheryavy, "Incorporating Bacterial Properties for Plasmid Delivery in Nano Sensor Networks," *IEEE Trans. on Nanotechnology*, vol. 14, pp. 751–760, July 2015.
- [22] S. Saha, K.C.-F. Leung, T. D. Nguyen, J. F. Stoddart and J. I. Zink, "Nanovalves," *Advanced Functional Materials*, vol. 17, no. 5, pp. 685693, March 2007.
- [23] S. M. Douglas, I. Bachelet, G. M. Church, "A Logic-Gated Nanorobot for Targeted Transport of Molecular Payloads," *Science*, vol. 335, February 2012.
- [24] F. Wu and C. Tan, "The engineering of artificial cellular nanosystems using synthetic biology approaches," *Wiley Interdisciplinary Reviews: Nanomedicine and Nanobiotechnology*, vol. 6, no. 4, pp. 369–383, July/August 2014.
- [25] I. F. Akyildiz, M. Pierobon, S. Balasubramaniam, and Y. Koucheryavy, "The internet of Bio-Nano things," *IEEE Communications Magazine*, vol. 53, no. 3, March 2015.
- [26] Z. Wang, K. Ng, Y. Chen, P. Sheu, and J. Tsai, "Simulation of bacterial chemotaxis by the random run and tumble model," *In Proc. IEEE BIBE*, pp. 228–233, Oct. 2011.
- [27] G. H. Weiss, "Aspects and applications of the random walk (Random materials and processes)," *North Holland Publishing Co.*, 1994.
- [28] W. Feller, "An introduction to probability theory and its applications: Volume 1," *Wiley*, 3rd edition, 1968.
- [29] M. A. Stephens, "EDF Statistics for Goodness of Fit and Some Comparisons," *J. of the American Stat. Assoc.*, vol. 69, pp. 730–737, 1974.
- [30] B. Levin, "Theoretical Aspects of Statistical Radiotechnics," *Soviet Radio*, 1969 (pages 155–157).
- [31] V. Petrov, "Sums of Independent Random Variables," *Springer-Verlag*, 1975.
- [32] M. Abramowitz, I. A. Stegun, "Handbook of Mathematical Functions with Formulas, Graphs, and Mathematical Tables," *New York: Dover*, 1965.
- [33] N. Smirnov, "Table for estimating the goodness of fit of empirical distributions," *Annals of Mathematical Statistics*, vol. 19, pp. 279–281, 1948.
- [34] P. Lio, S. Balasubramaniam, "Opportunistic routing through conjugation in bacteria communication nanonetwork," *Nanocommunication Networks (NANOCOMNET) Journal, Elsevier*, vol. 3, pp. 36–45, March 2012.
- [35] P. Doyle, L. Snell, "Random Walks and Electric Networks," *Mathematical Association of America*, 1984.
- [36] S. Redner, "A Guide to First-Passage Processes," *Cambridge University Press*, 2001.
- [37] W. Feller, "An introduction to probability theory and its applications: Volume 2," *Wiley*, 3rd edition, 1968.
- [38] P. E. Greenwood, M. S. Nikulin, "A Guide to Chi-Squared Testing," *Wiley-Interscience*, 1996.
- [39] V. Petrov, S. Balasubramaniam, R. Lale, D. Moltchanov, P. Lio, and Y. Koucheryavy, "Forward and reverse coding for chromosome transfer in bacterial nanonetworks," *Nanocommunication Networks (NANOCOMNET) Journal, Elsevier*, vol. 5, pp. 15–24, March-June 2014.
- [40] A. M. Cohen, "Numerical Methods for Laplace Transform Inversion," *Numerical Methods and Algorithms*, vol. 5., 2007.
- [41] T. Nakano, A. Eckford, and T. Haraguchi, "Molecular Communication," *Cambridge University Press*, 2013.